Journal of
Analytical & Bioanalytical Techniques

El-Wakil et al., J Anal Bioanal Tech 2014, 5:2
DOI: 10.4172/2155-9872.1000187

Research Article Open Access

Removal of Lead from Aqueous Solution on Activated Carbon and Modified Activated Carbon Prepared from Dried Water Hyacinth Plant

El-Wakil AM, Abou El-Maaty WM* and Awad FS

Chemistry Department, Faculty of Science, Mansoura University, Mansoura, Egypt

Abstract

In this work, the potential of activated carbon stems and leaves (ACS, ACL) prepared from dried water hyacinth stems and leaves (DS, DL) by chemical activation with phosphoric acid (1:3) and modified activated carbon stems and leaves (MACS, MACL) with nitric acid (1:1) for the removal of lead from aqueous solution was investigated. Carbon samples were produced with a reasonable yield about 75% and have a remarkable surface area (57.46, 71.83, 864.52, 493.78, 381.22, and 265.22 m^2/g for DS, DL, ACS, and ACL, MACS and MACL, respectively and well developed pore structure. Batch adsorption experiments were conducted to study the effect of various operating parameters, pH of the solution (1 to 6), initial concentration of lead ions (50 to 400 mg /l), contact time (2-250 min), and temperature (298-323 K). It is obvious that the maximum adsorption of lead at pH 5 is in the order: MACS (175.63 mg/g) > MACL (164.56 mg/g) > DS (90.50 mg/g) > DL (66.60 mg/g) > ACS (36.00 mg/g) > ACL (33.40 mg/g). This may be attributed to the increase in the number of active sites on the modified activated carbon. The equilibrium data were analyzed using Langmuir and Freundlich isotherms. The results showed that the experimental data were fitted well by the Langmuir model. Kinetic results revealed that the adsorption process obeyed a pseudo-second order model and intra-particle diffusion was the rate controlling step. The thermodynamic studies revealed that the adsorption was spontaneous and endothermic process. Desorption of about 90% of the sorbed lead from carbon was achieved using about 0.6 M HCl.

Keywords: Water hyacinth; Activated carbon; Modified activated carbon; Lead; Adsorption

Introduction

The removal of heavy metal contaminants from aqueous solutions is one of the most important environmental concerns because metals are bio refractory, and are toxic to many life forms. Various sources of heavy metals in water are battery manufacturing, basic steel, paper, pulp, metal plating, leather tanning, agrochemicals, petrochemicals, and chemical manufacturing, mining and fertilizer industries. Among the heavy metals, lead is one of the most toxic elements, even at low concentrations. It affects the central nervous system, kidney, liver, and gastrointestinal system, and it may directly or indirectly cause diseases such as anemia, encephalopathy, hepatitis, and the nephritic syndrome [1]. Because of the above factors, there is a necessity to remove these metals from wastewater in order to prevent contamination of natural water bodies by effluents containing toxic metals. The common methods for removing metal ions from water and wastewater include chemical precipitation, oxidation, reduction, reverse osmosis, membrane filtration and adsorption. Among the above methods, the promising process for the removal of metal ions from water and wastewater is adsorption, because the employed adsorbent can be regenerated by suitable desorption process and it is highly effective and economical [2].

Activated carbon is one of the most popular adsorbents for the removal of metal ions from aqueous solutions. Currently, activated carbon is widely used as an adsorbent in wastewater treatments. It has highly developed porosity, a large internal surface area, and relatively high mechanical strength. Despite its widespread use in industries, activated carbon remains an expensive material. Therefore, it is necessary to investigate and develop low-cost effective carbons that can be applied to water pollution control. The properties such as surface charge, type of surface functional groups, specific surface area, and pore-size distribution affect the adsorption capabilities of metal ions on activated carbon. All above mentioned physical and chemical properties of activated carbon depend on the precursor materials and activation methods used [3].

In this article, the possibility of using dried water hyacinth, Carbonized (stems, leaves) and modified Activated Carbon (stems and leaves) as efficient adsorbents for removal of Pb^{2+} from aqueous solution will be investigated. The effects of pH, initial Pb^{2+} concentration, and temperature and contact time on adsorption capacities were also examined. Experimental data were analyzed using first order kinetics, pseudo-second order kinetics and intra-particle diffusion model. Also, equilibrium isotherm data were analyzed according to Langmuir and Freundlich equations.

Experimental

Materials and reagents

Stock solution of Lead containing 1 mg lead cm^{-3} was prepared by dissolving 1.5984 g of $Pb(NO_3)_2$ (supplied by BDH) in distilled water and this solution was is completed up to the mark of 1 L measuring flask. Lead solutions of lower concentrations were prepared by further dilution with distilled water. PAR(2-pyridyl azo resorcinol) solution

***Corresponding author:** Dr. Weam Mahmoud Abou El-Maaty, Lecturer of Analytical Chemistry, Faculty of Science, P.O.Box: 35516, Mansoura University, Egypt, Tel: (+2) 01002582722–01099806635; Fax: (050) 2224132–2246254; E-mail: dr.weam_elmaaty@yahoo.com

Received February 21, 2014; **Accepted** March 28, 2014; **Published** March 31, 2014

Citation: El-Wakil AM, Abou El-Maaty WM, Awad FS (2014) Removal of Lead from Aqueous Solution on Activated Carbon and Modified Activated Carbon Prepared from Dried Water Hyacinth Plant. J Anal Bioanal Tech 5: 187 doi:10.4172/2155-9872.1000187

0.1% (w/v) prepared by dissolving 0.1 g of solid substance in least amount of distilled water then transfers to 100 ml measuring flask and complete to the mark using distilled water. All other chemicals used were of analytical grades.

Preparation of adsorbents

Preparation of dried water hyacinth (DS and DL): The plant water hyacinth was collected from Canal extended from river Nile in Mansoura, Egypt. The roots of the plant were removed while the leaves and stems were washed with water then with distilled water and were soaked in 0.25 M EDTA at pH 10 overnight for removing any metal ions adsorbed on the plant (stems and leaves) and washed with distilled water for several times and dried in oven at 110°C for 48 h then dried stems (DS) and leaves (DL) were ground and stored in desiccators till used in adsorption experiments.

Preparation of chemically activated carbon stems (ACS) and leaves (ACL): The dried phase was impregnated into 3 times its wt. with concentrated H_3PO_4 at room temperature for 2 days. then dried in oven at 110°C for 48 h then placed in a muffle oven (in a stainless steel reactor) where the samples were heated gradually in absence of air at a rate of heating=10 K/min up to 550-600°C and then maintained at this temperature for 3 h. After cooling to room temperature, the activated carbon obtained was washed thoroughly with distilled water until the pH of the supernatant become steady at about (pH=6). After that, the samples were dried at 110°C for 24 h. Finally, the Activated carbon prepared from stem (ACS) and leaves (ACL) were ground and stored in desiccators till used in adsorption experiments.

Modification of the activated carbon stems (MACS) and leaves (MACL): The activated carbon (ACS and ACL) were modified by surface oxidation with concentrated nitric acid (1:1 dilution from 67% concentrated HNO_3). The modification procedure was as follows. A known volume of 1:1 diluted nitric acid was heated at 110°C. The appropriate amount of ACS or ACL was added to the boiling nitric acid solution at a ratio of 1 g AC to 5 ml nitric acid solution. It was treated for 3 h to increase the formation of functional groups, such as carboxylic acids. The residual material was washed with distilled water until the pH of the supernatant become steady at about (pH=6). The modified activated carbon by using nitric acid was then dried at 120°C for 24 h and then were ground and stored in desiccators till used in adsorption experiments.

Batch adsorption experiments

Adsorption isotherms were studied by adding 0.025 g of DS, DL, ACS, ACL, MACS and MACL into 25 ml solutions with initial concentrations of Pb (II) ranging from 5 to 400 mg/L. The initial pH values of the solution were 5. After the suspensions were shaken for 2 h, the remaining concentrations of Pb (II) was analyzed by measuring the absorption of the respective PAR (2-pyridyl azo resorcinol) complex (PAR–Pb) at 520 nm employing a modification of the method proposed by Dagnall et al. [4]. Specifically, 10 ml of buffer solution (borate buffer pH=10) was added to metal solution followed by addition of 1 ml PAR (0.1 g/100 ml), then complete to 25 ml using distilled water. The amounts of Pb^{2+} removed by sorbents q_e and percent extracted %E can be calculated using the following equations:

$$Extraction\% = \frac{(C_O - C_e)}{C_O} \times 100 \quad (1)$$

$$q_e = \frac{(C_O - C_e)V}{m} \quad (2)$$

Where q_e is the amount of Pb^{2+} adsorbed (mg/g). C_o and C_e are the initial and equilibrium liquid-phase concentrations of Pb^{2+} (mg/g), respectively. V is the volume of the solution (L), and m is the weight of the sorbent used (g).

To study the effects of pH on Pb (II) adsorption, 0.025 g of the adsorbent were dispersed into 25 ml solutions containing 250 mg/L of Pb(II). The initial pH values of the solutions were adjusted from 1.5 to 6 using 0.01 M HNO_3 and 0.01 M NaOH.

Kinetic experiments were performed by using different flasks containing around 0.2 g of adsorbent in 200-ml solutions containing 200 mg/L of Pb^{2+}. At desired time intervals, 1 ml of aliquots were taken from the suspension and the concentration of Pb^{2+} is determined spectrophotometrically as described above.

Result and Discussion

Characterization of prepared samples

Physic-chemical characterization of MACS, MACL, ACS, ACL, DS and DL were determined as follow: moisture content determined using oven drying method, point of zero charge (pH_{pzc}), surface area was determined from the application of Brunauer Emmett and Teller (BET) equation to the adsorption-desorption isotherm of N_2 at 77k [5], as shown in (Table 1). The morphology of MACS, MACL, ACS, ACL, DS and DL examined by electron microscopy is shown in Figure 2. Examination of SEM micrographs obtained clearly indicate the porous structure of different adsorbents at magnification of 1500x, 3500x and 1000x for (DS and DL), (ACS and ACL) and (MACS and MACL), respectively. The FT-IR spectra for similar samples are shown in Figure 1. All samples show wide band at about (3373-3442 cm^{-1}) due to O-H stretching mode of hexagonal group and adsorbed water. The shoulders observed at (2849-2932 cm^{-1}) due to aliphatic (C-H) and appear for all samples [6].The bands near 1600 cm^{-1} is due to C=C stretching vibration in aromatic ring and is observed for all samples. The bands at (1711-1713 cm^{-1}) for MACL and MACS are due to stretching vibration of carboxyl groups on the edges of layer plane [7]. The weak bands appearing at 1580, 1574, 1240, 1520, 1608, 1243, 1530 and 1621 cm-1 are due to formation of highly conjugated (C=O stretching, C-O stretching in carboxylic groups and carboxylate moieties.) [8].

Adsorption parameters

Effect of pH: To optimize the pH for maximum removal efficiency and to avoid the precipitation of Pb (II), a sorption experiment was conducted in the initial pH range from 2 to 6, as shown in Figure 3. The amount adsorbed by DS increased from 21.04 to 102.50 mg/g, for sample DL from 17.10 to 68.04 mg/g, for sample ACS from 1.30 to 35.80 mg/g and for sample ACL from 0.6 to 32.30 mg/g at pH=1 and 5, respectively. At low pH, the surface of the adsorbent was surrounded by hydronium ions that compete with metal ions, which prevented the metal ions from approaching the binding sites on the adsorbent.

Samples	Moisture content %	Surface pH	Surface Area m^2/g	Total pore volume	pH PZC
DS	6.71	5.95	57.46	0.01	4.95
DL	5.1	6.13	71.83	0.03	4.80
ACS	3.88	4.50	864.52	0.52	4.05
ACL	2.64	4.10	493.78	0.31	4.05
MACS	9.13	3.60	381.22	0.43	3.38
MACL	7.89	4.00	365.22	0.29	3.36

Table 1: Characteristics of the dried Water hyacinth (stems and leaves), activated carbon and modified activated carbon (stems and leaves).

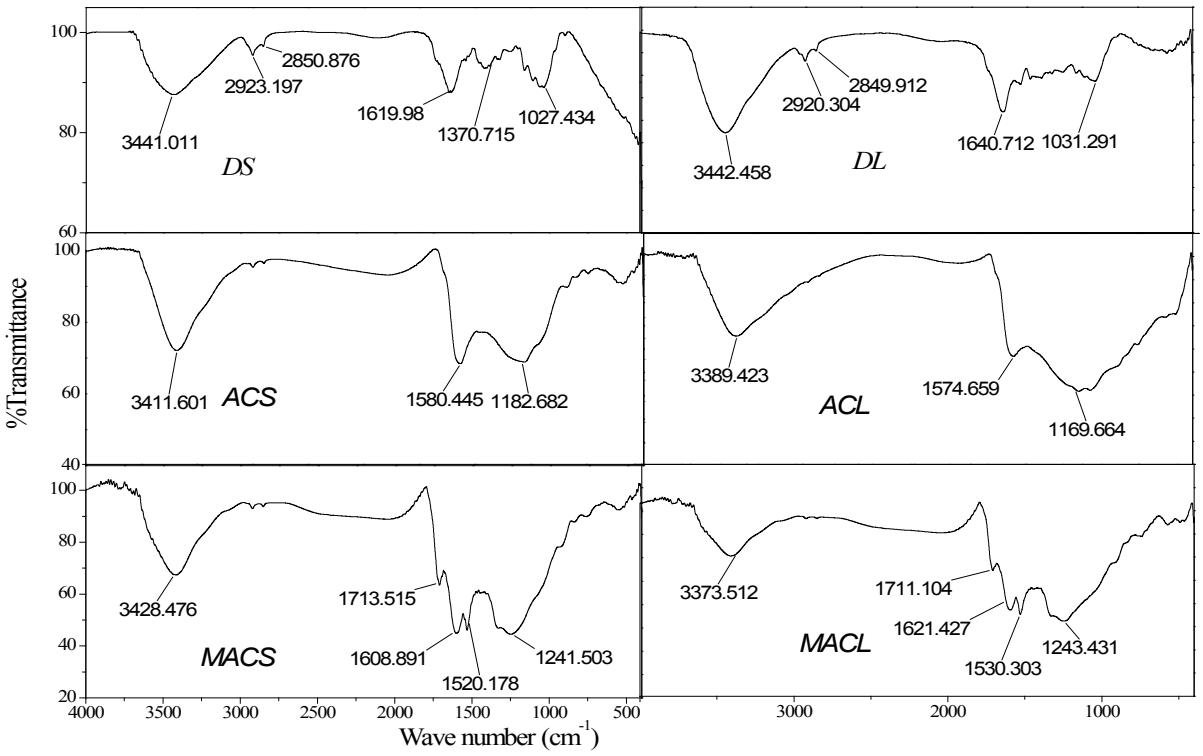

Figure 1: FTIR spectrum of dried Water hyacinth (stems and leaves), activated carbon and modified activated carbon.

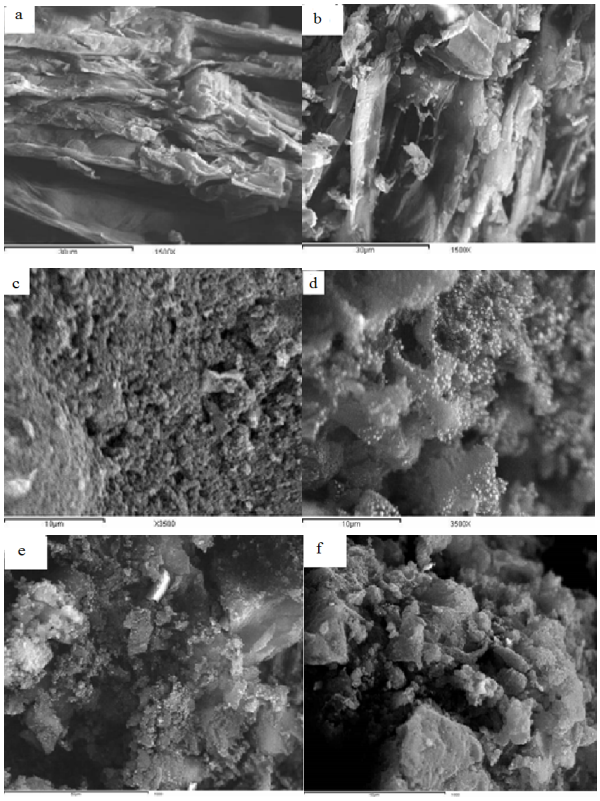

Figure 2: SEM photographs of (a) DS (b) DL (c) ACS (d) ACL (e) MACS (f) MACL.

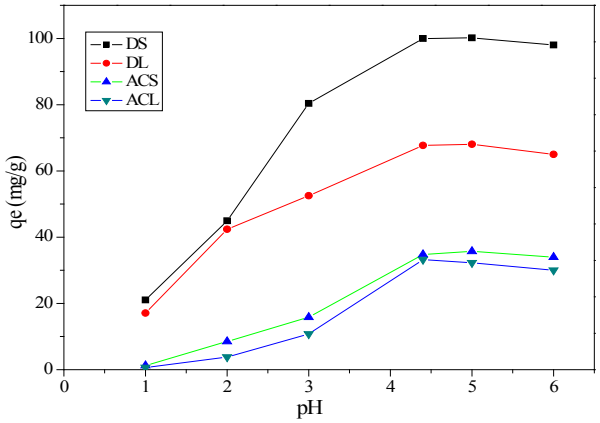

Figure 3: Effect of the pH values on adsorption capacity of Pb^{2+} by DS, DL, ACS and ACL (Conditions: C_0=250 mg/l, T=25°C; adsorbent dose=0.025 g/25 ml).

The increase in metal removal as pH increases can be explained on the basis of a decrease in competition between hydronium ions and metal species for the surface sites. At pH=5.0, the adsorption capacity of (DS, DL, ACS and ACL) almost reaches the maximum value. Because the speciation diagram of lead shows that at pH>6.0 the species such as $[Pb(OH)]^+$, $[Pb3(OH)4]^+$, and $[Pb(OH)_2]$ will be produced [9]. In order to guarantee to truly examine the adsorption property of carbon samples as well as to avoid precipitation of Pb(II) ions, all the following experiments were conducted at pH=5.0.

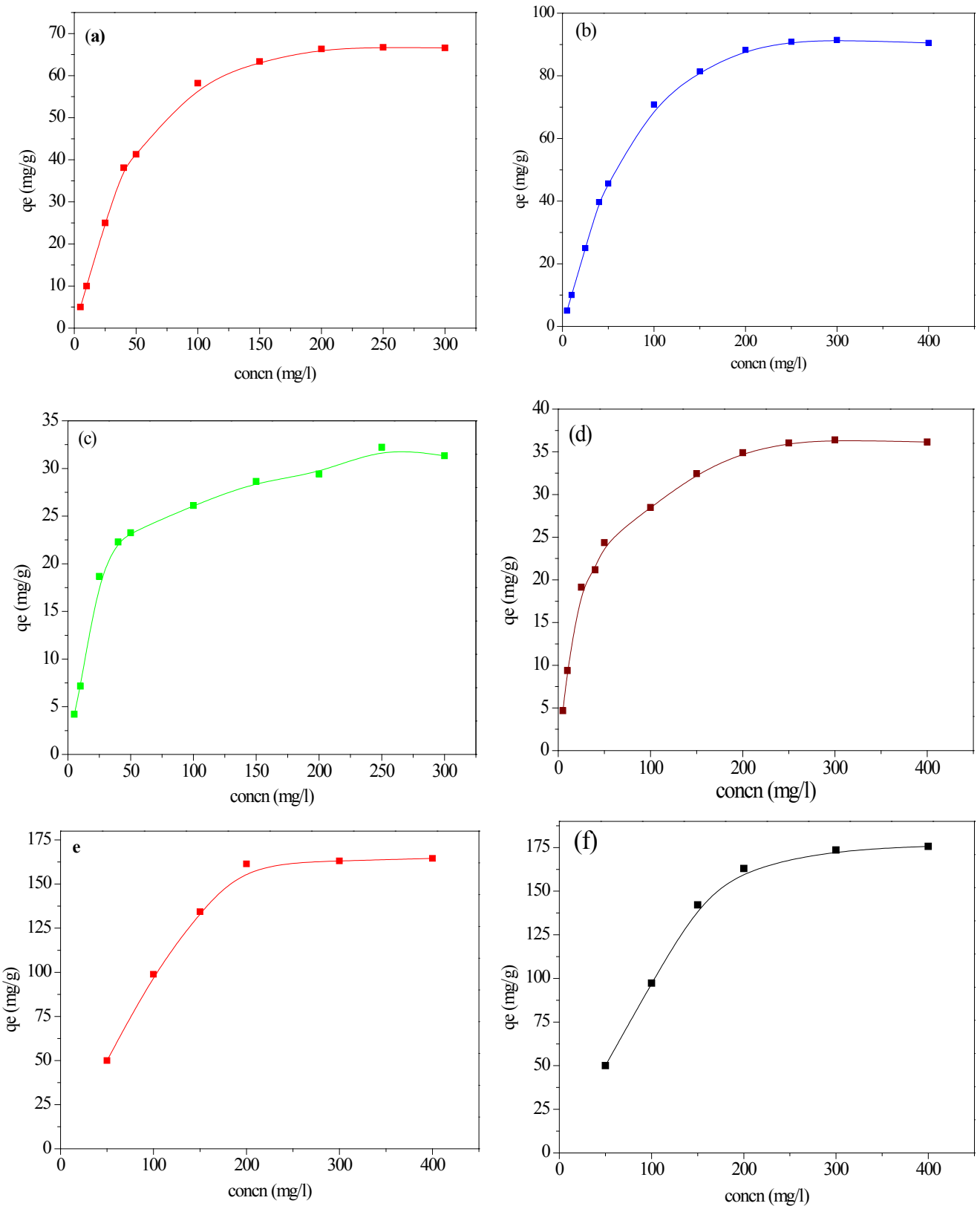

Figure 4: Effect of initial metal concentration on the removal of Pb^{2+} by(a)DL, (b)DS, (c) ACL, (d) ACS, (e) MACL and (f)MACS.(Conditions: C_0=50-400 mg/l, T=25°C; adsorbent dose=0.025 g/25 ml).

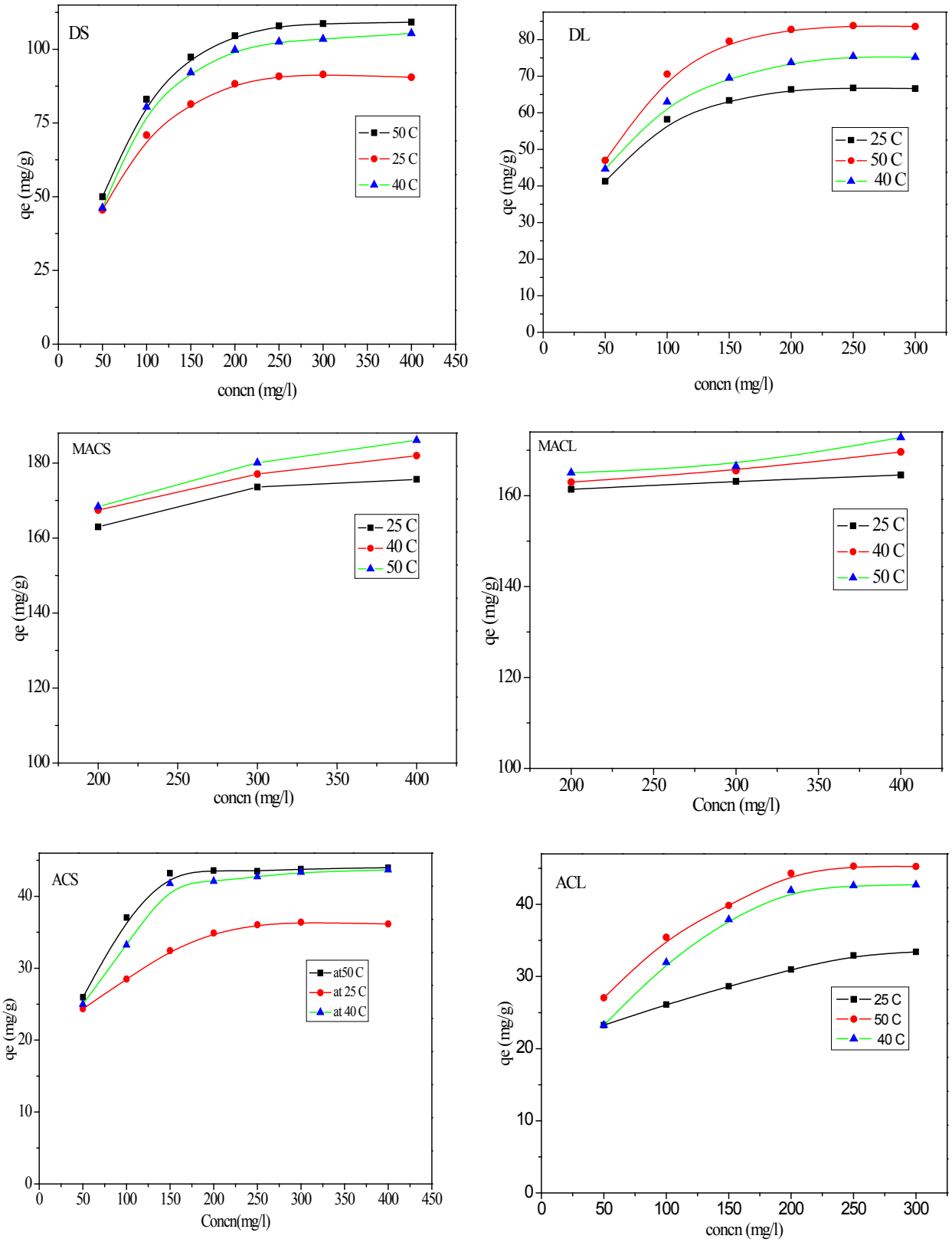

Figure 5: Effect of temperature on adsorption capacity of Pb^{2+} by DS, DL, ACS, ACL, MACS and MACL (Conditions: C_0=50-400 ppm; adsorbent dose=0.025 g/25 ml).

Effect of initial concentration on the uptake of pb^{2+}

The effect of initial concentration on adsorption was investigated, as illustrated in Figure 4 and 5. It is revealed that, as the initial concentration increased, the adsorption capacities increased. The initial concentration may provide the driving force to overcome the resistance of the mass transfer of Pb(II) between liquid and solid phases [10]. The initial concentration was higher, and then the driving force was higher, and therefore the adsorption capacity would be higher.

Effect of temperature on adsorption

The effect of solution temperature on Pb^{+2} removal was studied at three different temperatures: 298 K, 313 K and 323 K using DS, DL, ACS, ACL, MACS and MACL. The results are presented in Table 2, and it is obvious from the table that increasing the temperature significantly affected the amount of Pb^{2+} adsorbed from solution by different adsorbents. The enhancement in the adsorption capacity might be due to the chemical interaction between adsorbate and adsorbent sites or the increased rate of intra particle diffusion of Pb^{2+} molecules into the pores of the adsorbents as a result of decreasing solution viscosity at higher temperatures and the number of adsorption sites generated because of some internal bonds near the edge of surface active sites of sorbent [11,12].

Samples	*Qe (mg g⁻¹)*		
	298 K	*313 K*	*323 K*
DS	90.50	105.37	109.17
DL	66.60	75.14	83.54
ACS	36.00	43.00	44.00
ACL	33.40	42.72	45.25
MACS	175.63	181.96	186.07
MACL	164.56	169.62	172.79

Table 2: Effect of temperature on maximum adsorption capacities of Pb2+ be DS, DL, ACS, ACL, MACS and MACL.

Effect of contact time on adsorption

Figure 6 shows the effect of contact time on the percent removal of Pb^{2+} by (a) DS and DL, (b) ACS and ACL, (C) MACS and MACL at 25°C using a sorbent concentration of 1 g/L at pH 5. The initial concentration of Pb^{2+} was 200 ppm. It is obvious that, the adsorption amount of Pb(II) rapidly increased at the beginning of adsorption; more than 65% of the adsorption capacities of corresponding adsorbents for Pb^{2+} occurred within 5 min for DS and DL and more than 88% occurred within 5 min for ACS and ACL and about 90% occurred within 15 min for MACS and MACL. Pb^{2+} uptake almost remained constant after 60 min for MACS, MACL, ACS and ACL and after 90 min for DS and DL so 90 min could be considered the equilibrium time of the Pb (II) adsorption. The fast adsorption at the initial stage may be due to the higher driving force making fast transfer of metal ions to the surface of adsorbent particles and the availability of the uncovered surface area and the active sites on the adsorbent.

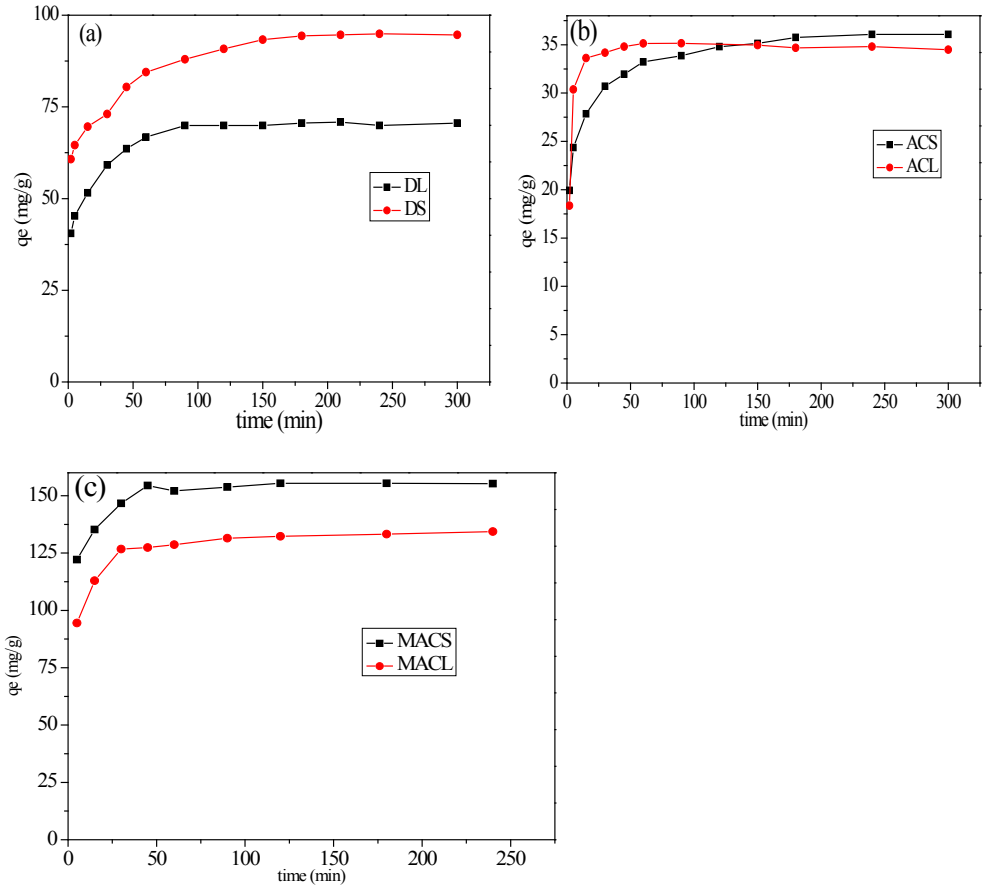

Figure 6: Effect of contact time on adsorption capacity of Pb^{2+} by (a) DS and DL (b) ACS and ACL,(C)MACS and MACL. (Conditions: C_0=250 mg/l, T=25°C; adsorbent dose=0.2 g/200 ml).

Effect of adsorbent dosage

The effect of amount of DS, DL, ACS and ACL on the removal percentage of Pb^{2+} was shown in Figure 7. It could be clearly seen that, an increase in sorbent dose is in favor of Pb^{2+} removal. When the sorbent dose increases from 0.05 to 0.25 g, the percent Pb^{2+} removal by DS, DL, ACS and ACL increase from 48.40% to 96.36 %, from 31.01% to 95.63% , from 17.9 % to 53.95% and from 16.46% to 50.95%, respectively. Increase in adsorption with adsorbent dosage can be attributed to increased adsorbent surface area and availability of more adsorption sites.

Adsorption isotherms

Adsorption is usually described through isotherms, that is, the amount of adsorbate on the adsorbent as a function of its pressure (if gas) or concentration (if liquid) at constant temperature. Adsorption isotherm is important to describe how adsorbates interact with adsorbents and so it is important in optimizing the use of adsorbents. Two common isotherm equations namely, Langmuir and Freundlich models were tested [13-15].

The Langmuir isotherm assumes a surface with homogeneous binding sites equivalent sorption energies, and no interaction between adsorbed species. Its mathematical form is written as:

$$\frac{C_e}{q_e} = \frac{1}{Q_b} + \frac{C_e}{Q} \quad (3)$$

Where q_e is the amount adsorbed at equilibrium (mg g^{-1}), C_e is the equilibrium concentration of the lead (mg L^{-1}), constant b is related to the energy of adsorption (Lmg^{-1}), Q is the Langmuir monolayer adsorption capacity (mg g^{-1}). The essential characteristics of the Langmuir equation can be expressed in terms of a dimensionless separation factor RL.

$$R_L = \frac{1}{1 + bC_o} \quad (4)$$

C_0 is the highest initial solute concentration, b is Langmuir adsorption constant (L/mg), RL indicates the type of isotherm to be reversible (RL=0), Favorable (0<RL>1), Linear (RL=1) or unfavorable (RL>1) [16].

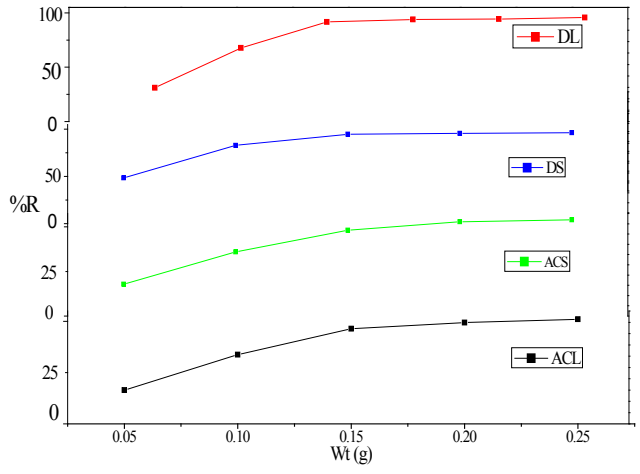

Figure 7: Effect of sorbent dosage on the removal of Pb^{2+} by DS, DL, ACS and ACL. (Conditions: T=25°C; C_0=200 mg/l, v=50 ml; time=7 h).

Adsorbents	Langmuir parameters				
	R^2	b (L/mg)	$Q_{max^2\ fitted}$	$Q_{exp,}$	R_L
MACS	0.999	0.555	176.700	175.630	0.005
MACL	0.999	0.741	165.300	164.557	0.003
ACS	0.998	0.071	37.780	36.000	0.034
ACL	0.994	0.086	33.990	33.400	0.086
DS	0.999	0.199	92.170	90.500	0.012
DL	0.999	0.221	68.070	66.600	0.016

Table 3: Parameters of langmuir isotherm for adsorption of Pb^{2+} by DS, DL, ACS, ACL, MACS and MACL.

Adsorbents	Freundlich parameters		
	R^2	K_f	1/n
MACS	0.773	97.710	0.121
MACL	0.894	101.510	0.099
ACS	0.992	13.900	0.175
ACL	0.987	14.040	0.153
DS	0.926	37.880	0.168
DL	0.948	33.860	0.132

Table 4: Parameters of Freundlich isotherm for adsorption of Pb^{2+} by DS, DL, ACS, ACL, MACS and MACL.

The Freundlich isotherm is an empirical equation based on an exponential distribution of adsorption sites and energies. It is represented as:

$$\ln q_e = \ln K_f + \frac{1}{n} \ln C_e \quad (5)$$

Where q_e is the amount adsorbed at equilibrium (mg g^{-1}), C_e is the equilibrium concentration of lead (mg L^{-1}), K_f is roughly an indicator of the adsorption capacity, and 1/n is the adsorption intensity. A linear plot of ln q_e versus ln C_e confirms the validity of the Freundlich model.

Figures 8 and 9 show the linear plot of Langmuir and Freundlich isotherms for adsorption of Pb^{2+} on DS, DL, ACS, ACL, MACS and MACL. The model parameters obtained by applying Langmuir and Freundlich models to the experimental data are given in Tables 3 and 4. It can be found that the regression coefficients R2 obtained from Langmuir model are closer to 1 than that of the Freundlich model, suggesting that the Langmuir isotherm fits better with the adsorption of Pb^{2+} on DS, DL, ACS, ACL, MACS and MACL. In addition, the q_{max} values for the adsorption of Pb^{2+} onto the different adsorbents calculated from the Langmuir model are all the same as the experimental data. Also, RL values obtained are in the range of (0.000-0.086), thereby confirming that the adsorption is a favorable process. It can be concluded that the monolayer Langmuir adsorption isotherm is more suitable to explain the adsorption of Pb^{2+} onto different adsorbents.

Adsorption kinetics

The pseudo-first order equation and the pseudo-second order equation: In order to investigate the controlling mechanism of adsorption process of Pb^{2+} by DS, DL, ACS, ACL, MACS and MACL, the pseudo-first order and the pseudo-second order kinetic models were cited to evaluate the experimental data. The pseudo-first order kinetic model has been widely used to predict metal adsorption kinetics. It was suggested by Lagergren [17] for the adsorption of solid/liquid systems. The differential form of the pseudo-first order model of adsorption can be expressed as:

$$\frac{dq_t}{dt} = k_1(q_e - q_t) \quad (6)$$

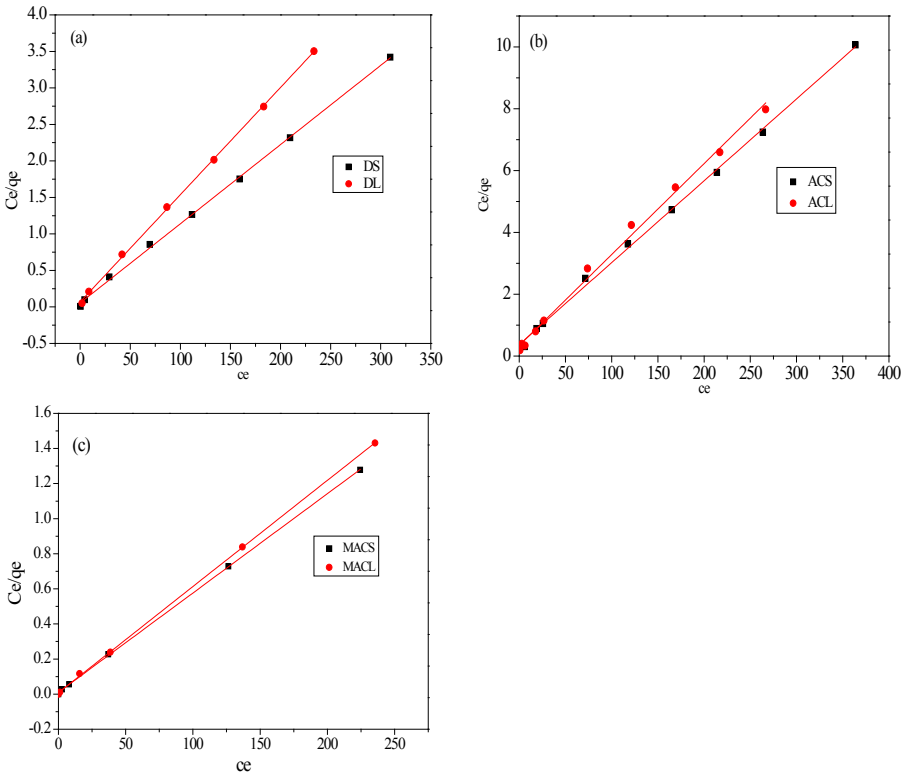

Figure 8: Langmuir plot for the adsorption of Pb^{2+} by (a) DS, DL (b) ACS, ACL (C) MACS, MACL.

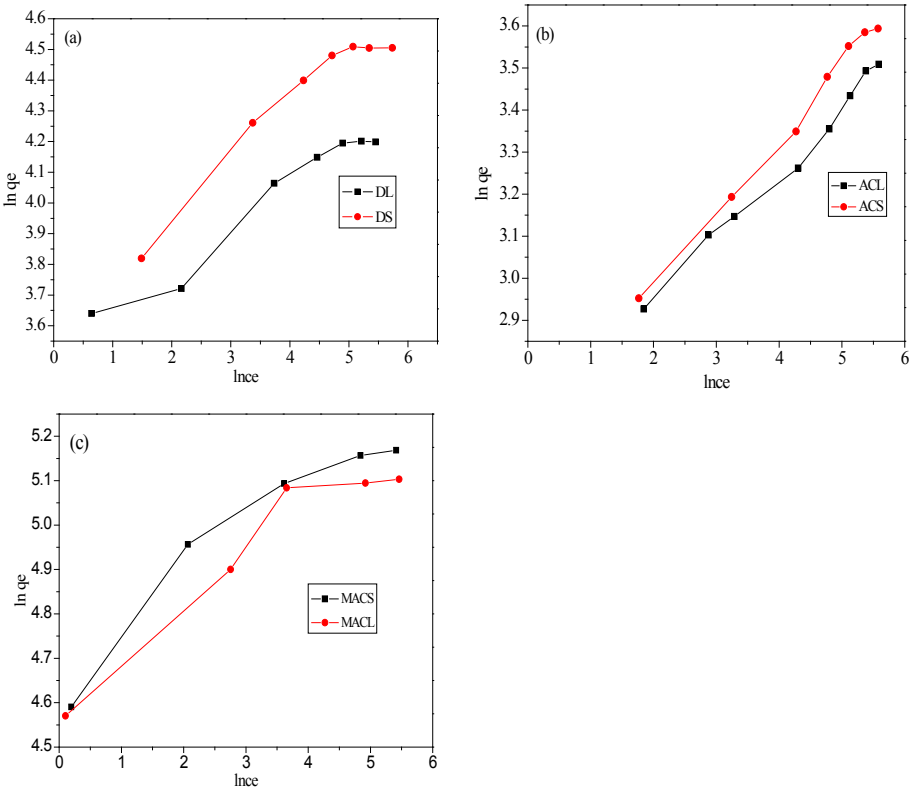

Figure 9: Freundlich plot for adsorption of Pb^{2+} by a) DS,DL (b) ACS, ACL (C) MACS, MACL.

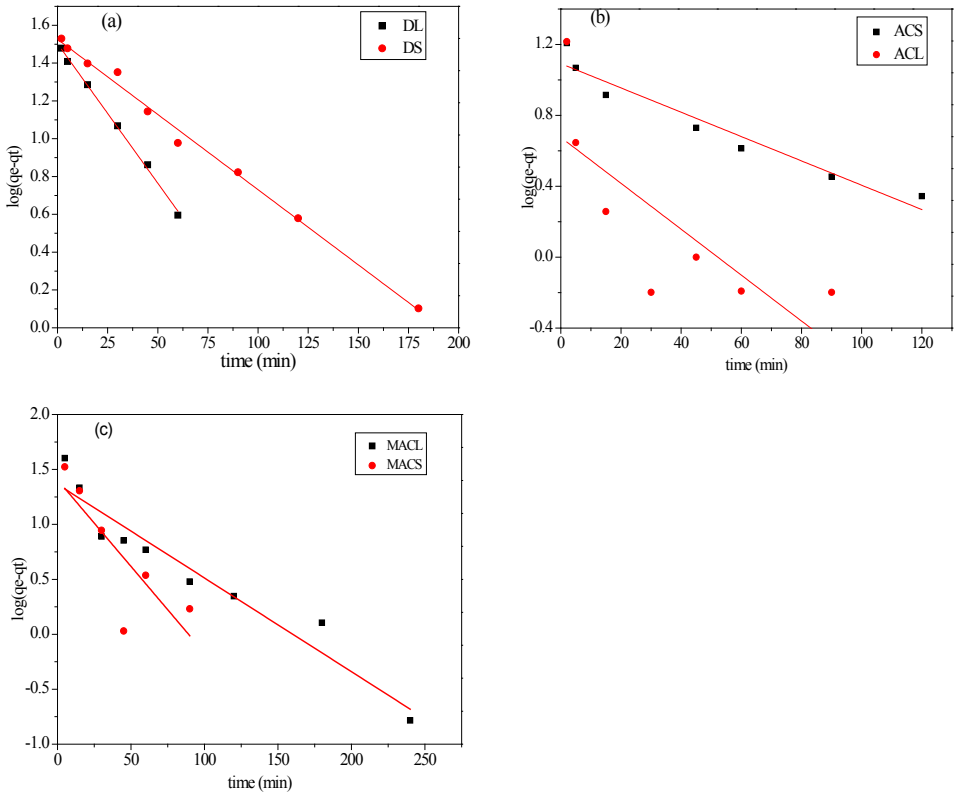

Figure 10: Pseudo-first-order kinetic Model for the adsorption of Pb^{2+} by (a) DS, DL (b) ACS, ACL and (c) MACS, MACL.

Adsorbent Code	$q_{e\ exp.}$ mg.g^{-1}	$q_{e\ cal.}$ mg.g^{-1}	K_1 (min^{-1})	R^2
MACS	155.5	4.08	0.036	0.600
MACL	134.0	3.92	0.019	0.925
ACS	35.0	2.98	0.213	0.929
ACL	33.0	1.97	0.029	0.511
DS	92.0	3.53	0.018	0.993
DL	70.6	4.49	0.034	0.997

Table 5: Parameters of first order model for adsorption of Pb^{2+} by DS, DL, ACS, ACL, MACS and MACL.

Adsorbent Code	$q_{e\ exp.}$ mg.g^{-1}	$q_{e\ cal.}$ mg.g^{-1}	K_2 g. mol^{-1} .min^{-1}.	R^2
MACS	155.5	156.49	0.041	0.999
MACL	134.0	135.50	0.027	0.999
ACS	35.0	35.34	0.009	0.998
ACL	33.0	35.84	0.002	0.999
DS	92.0	94.69	0.020	0.996
DL	70.6	72.31	0.003	0.999

Table 6: Parameters of second order kinetic model for adsorption of 200 ppm Pb2+ by DS, DL, ACS, ACL, MACS and MACL.

Where q_e and q_t (mg/gm) are the amounts of lead adsorbed at equilibrium and at time t, respectively and k_1 is the equilibrium constant (min^{-1}). Integration of equation (6) and by applying the initial conditions qt = 0 at t= 0 and the linear form can be formulated as [18]:

$$\log(q_e - q_t) = \log q_e - \frac{K_1 t}{2.303} \quad (7)$$

Where q_e is the adsorption uptake of Pb^{2+} at time t (mg/g) and k_1 (min^{-1}) is the rate constant of the pseudo-first-order adsorption. A plot of log (q_e-q_t) versus *t* should be linear; the parameters k1 and R^2 (correlation coefficient) calculated from the data (Figure 10) are listed in Table 5. It can be seen that the linear correlation coefficients (R^2) for the pseudo-first order kinetic model are high. However, there are large differences between the experimental q_e values ($q_{e,exp}$) and the calculated q_e values ($q_{e,cal}$), which indicated the pseudo-first order kinetic model was poor fit for the adsorption processes of DS, DL, ACS, ACL, MACS and MACL for Pb^{2+}.The differential form of the pseudo-Second order reaction equation may be written as [18,19]: [9]

$$\frac{dq_t}{d_t} = k_2 (q_e - q_t)^2 \quad (8)$$

After integration considering the boundary conditions the linearized form of this model can be expressed as [18]

$$\frac{t}{q_t} = \frac{}{K\ q_e} + \frac{t}{q_e} \quad (9)$$

Where k_2 (g mol^{-1} min^{-1}) is the rate constant of pseudo-second-order adsorption. Figure 11 shows the plot of t/q versus t for Pb^{2+} onto DS, DL, ACS, ACL, MACS and MACL. It can be observed from Table 6 that R^2 values for the pseudo-second order kinetic model are all over 0.999, moreover, the $q_{e,cal}$ values for the pseudo-second order kinetic model are all consistent with the $q_{e,exp}$ values. These suggested that the adsorption processes of DS, DL, ACS, ACL, MACS and MACL for Pb^{2+} can be well described by the pseudo-second order kinetic model. These suggested that the pseudo-second-order adsorption mechanism was predominant referring that adsorption process is controlled by chemisorption which involves valence forces through sharing or

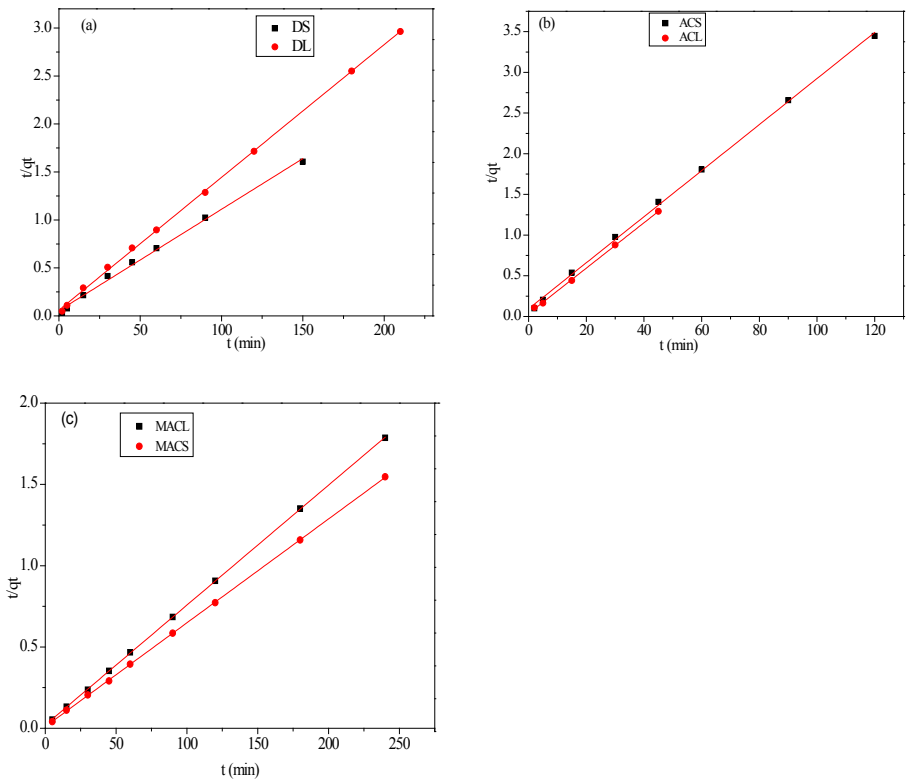

Figure 11: Pseudo-second-order model for the adsorption of Pb^{2+} by (a) DS, DL (b) ACS, ACL and (c) MACS, MACL.

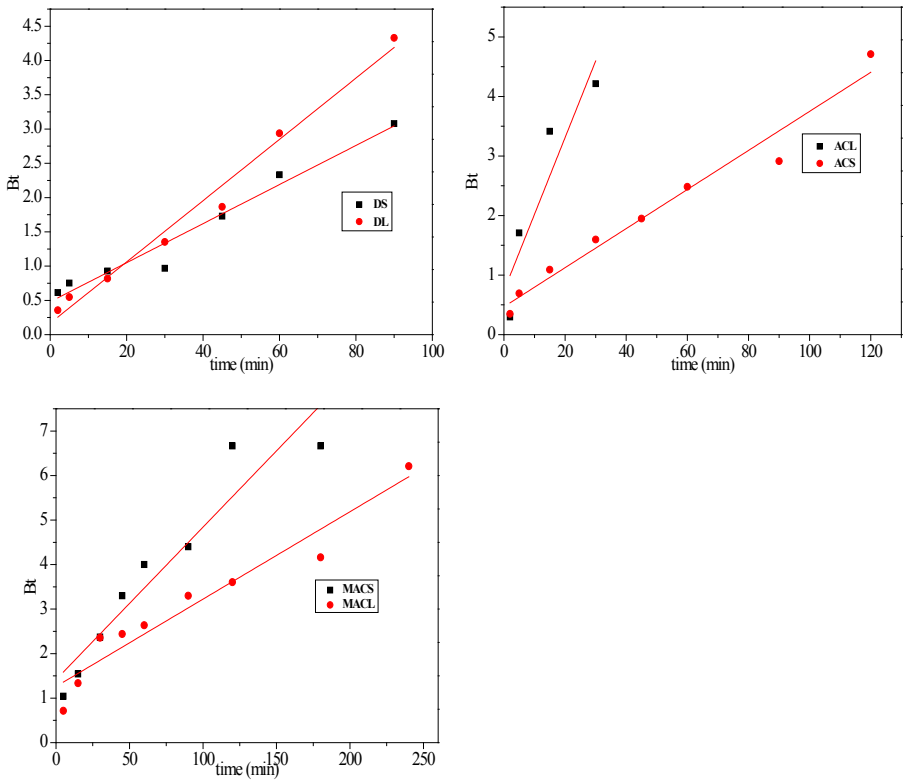

Figure 12: Bt versus t plot for adsorption of Pb^{2+} on DS, DL, ACS, ACL, DL, MACS, MACL at 200 ppm.

exchange of electron between the solvent and the adsorbate Since neither the pseudo-first-order nor the second-order model can identify the diffusion mechanism, the kinetic results were further analyzed by the intra-particle diffusion mode to elucidate the diffusion mechanism.

Intra-particle diffusion model: Adsorption is a multi-step process involving transport of solute molecules from the aqueous phase to the surface of the solid particles of adsorbent, and then diffusion of the solute molecules into the interior of the pores, which is likely to be a slow process, and is therefore, rate determining. The intra-particle diffusion parameter, K_d ($mg.g^{-1}$ $h^{-0.5}$) is defined by the following equation [20]:

$$q_t = K_d t^{0.5} + C \quad (10)$$

Where k_d is the intra-particle diffusion rate constant ($mg.g^{-1}$ $h^{-0.5}$) and C is a constant. According to this model qt versus $t^{0.5}$ should be linear if intra-particle diffusion is involved in the adsorption process. From Eq. (10), if pore diffusion is the rate limiting step, then a plot of q_t against $t^{0.5}$ must give a straight line with a slope that equals k_d and the intercept value C represents the resistance to mass transfer in the external liquid film.

Intraparticle diffusion model				*Boyd model*	
Adsorbent code	***R²***	***K_p (mg g^{-1} $min^{-0.5}$)***	***Intercept***	***Intercept***	**R2**
MACS	0.563	2.089	130.320	0.034	0.89
MACL	0.590	2.373	104.373	1.261	0.925
ACS	0.872	0.656	27.039	0.468	0.964
ACL	0.520	0.640	30.142	0.788	0.735
DS	0.954	2.874	58.700	0.479	0.958
DL	0.975	3.764	36.848	0.167	0.982

Table 7: Intraparticle diffusion parameters for adsorption of Pb(II) by DS, DL, MACS and MACL at 200 ppm.

Figure 12 shows the plot of q_t against $t^{0.5}$ for adsorption of 200 ppm Pb^{2+} by DS, DL, ACS, ACL, MACS and MACL, the plots are multi linear, containing at least three linear segments which indicate that three steps occur during adsorption process. The first sharper portion is transport of Pb^{2+} from the bulk solution to the adsorbent external surface by diffusion through the boundary layer (film diffusion). The second portion is the diffusion of Pb^{2+} from the external surface into the pores of the adsorbent. The third portion is the final equilibrium stage, where Pb^{2+} were adsorbed on the active sites on the internal surface of the pores and the intra- particle diffusion starts to slow down due to the solute concentration getting lower and lower in solution In addition, the linear portions of curves did not pass through the origin suggesting that pore diffusion is not the step controlling the overall rate of mass transfer at beginning of adsorption.

In Table 7, the correlation coefficients (R^2) for the linear segment intra-particle diffusion model were between 0.563 and 0.975, indicating that the intra-particle diffusion was not the only rate-controlling step; other process could control the rate of adsorption. The boundary layer effect may control the rate of mass transfer in the time period of the first linear segment; this conclusion could be corroborated by the analysis of data from Boyd's model.

The model of Boyd is expressed as [21]:

$$F = 1 - \frac{6}{\pi^2}\exp(1 - Bt) \quad (11)$$

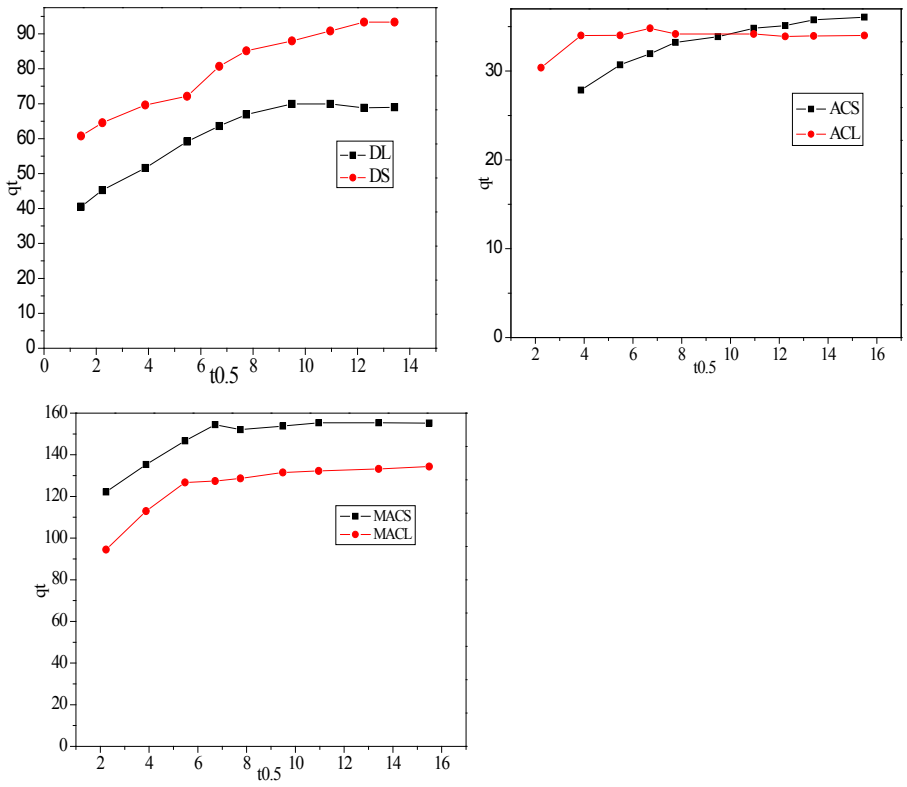

Figure 13: Intra-particle diffusion plots for adsorption of Pb^{2+} on DS, DL, ACS, ACL, MACS, MACL at 200 ppm.

Where F is the fractional attainment of equilibrium, at different times, t, and Bt is a function of F.

$$F = \frac{q_t}{q_e} \quad (12)$$

Where q_t and q_e are the metal uptake (mmol g^{-1}) at time t and at equilibrium, respectively.

Equation (18) can be rearranged to [22]

$$B_t = -0.4977 - \ln(1-F) \quad (13)$$

Figure 13 shows the values of B_t were calculated from Eq. (13) and plotted against time t. The linearity of this plot can provide available information to distinguish intra-particle diffusion and boundary layer effect (film diffusion) rates of adsorption. If a plot of B_t versus t is a straight line passing through the origin, then adsorption will fit layer effect. The plots are linear only in the initial period of adsorption and do not pass through the origin, indicating that external mass transfer is the rate limiting process in the beginning of adsorption and then is the intra- particle diffusion.

Thermodynamic study

The data obtained from the temperature study were used for thermodynamic analysis. Thermodynamic parameters such as change in standard free energy (ΔG°), enthalpy (ΔH°), and entropy(ΔS°) were determined using the following eqs [23]:

The van't Hoff equation

$$\ln k_d = \frac{\Delta S}{R} - \frac{\Delta H}{RT} \quad (14)$$

$$\Delta G° = \Delta H° - T\Delta S° \quad (15)$$

$$Kd = \frac{q_e}{c_e} \times \rho \quad (16)$$

Where K_d is the adsorption coefficient, ρ=1000 g/L to make adimensionles Kd [24], ΔG° (J/mol) is the change in Gibbs Free Energy, ΔH°(J/mol) is the enthalpy change of Pb^{2+} adsorption, ΔS° (J/molK) is the entropy change of Pb^{2+} adsorption, R is the universal gas constant (8.314 J/mol K) and T is the absolute temperature (K).

By plotting a graph of ln K_d versus 1/T (Figure 14), the values of ΔH° and ΔS° can be estimated from the slope and intercept of van't Hoff plots, respectively. The thermodynamic parameters are given in Table 8. It is clear from the table that the values of ΔG° are negative for DS, DL, ACS, ACL, MACS and MACL. The negative values of ΔG° at various temperatures indicate the spontaneous nature of the sorption process. The fact that the values of the ΔG° decrease with increasing temperature indicates the increase of spontaneous effect. For all the sorbents, the positive value of ΔH° suggested the endothermic nature of the adsorption process. Moreover, the positive values of ΔS° point out the increased randomness at the solid/liquid interface during the sorption of Pb^{+2} by DS, DL, ACS, ACL, MACS and MACL.

Desorption studies

To achieve practical and economical adsorption, a promising adsorbent is required to have not only high adsorption capacity but also regeneration ability for recycling use. The use of thermal activation to regenerate the adsorbent could require high energy and result in a 5-10% adsorbent loss in each cycle. Hence, Studies were attempted to use chemical regeneration for adsorbate desorption [25]. Desorption of Pb using HCl as a desorping agent by disruption coordination of metal ions and subsequent release from the activated carbon surface into the desorption medium was studied. In order to investigate the desorption capacity of different adsorbents, 0.025 g of different adsorbents were introduced to 25 ml solution of 200 ppm of lead at pH 5. As the adsorption reaches equilibrium, the metal ion concentration of the solution was measured, Then, the adsorbent loaded with lead was collected and treated with 25 ml×M HCl to remove the adsorbed Pb^{2+}. The results relating to desorption of lead by HCl of different concentration are shown in Tables 9 and 10. The results show that increase in concentration of HCl. The desorption also increased but remained constant with 0.6 M HCl.

Comparison of the adsorption capacities of sorbents toward Pb^{2+}

Table 11 lists the comparisons of maximum adsorption capacities of Pb^{2+} on DS, DL, ACS, ACL, MACS and MACL obtained in this study with various adsorbents previously used for the adsorption of Pb^{2+} [26,27]. The MACS and MACL have a higher adsorption capacity than that of the most other adsorbents reported in the literature, suggesting that it may be potential for Pb^{2+} removal from aqueous solution.

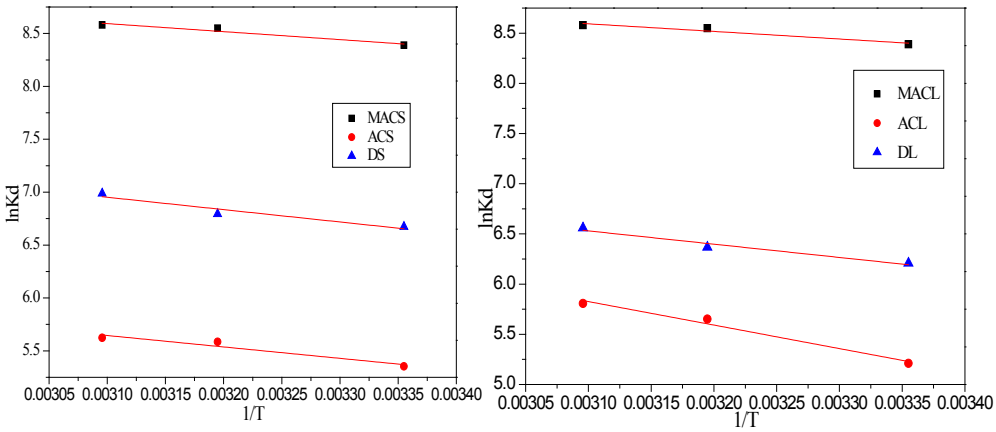

Figure 14: The plots of lnKd versus T^{-1} for estimations of thermodynamic parameters of the adsorption process of Pb^{2+} by MACS, MACL, ACS, ACL, DS and DL. Condition :(C_0=200 ppm, T= 25–50°C, t=7 h, adsorbent dose=0.025 g/25 ml).

Adsorbent Code	ΔH° (KJ/mol)	ΔS° (KJ/mol K)	ΔG° (KJ/mol)		
			298 K	308 K	318 K
MACS	14.599	0.091	-12.49	-13.85	-14.76
MACL	16.284	0.100	-13.52	-15.02	-16.00
ACS	8.970	0.075	-13.49	-14.63	- 15.38
ACL	11.190	0.109	-21.29	-22.93	-24.02
DS	9.710	0.088	-16.51	-17.83	-18.71
DL	10.990	0.088	-15.35	-16.67	-17.56

Table 8: Thermodynamic parameters for adsorption of Pb^{2+} by MACS, MACL, ACS, ACL, DS and DL at different temperatures.

Adsorbent code	q_e adsorbed	q_e desorped	% desorption
MACS	155.0	81.49	52.57
MACL	134.0	76.58	57.15
ACS	33.9	18.70	55.08
ACL	30.9	21.04	68.10
DS	88.2	50.00	56.70
DL	64.7	49.52	76.55

Table 9: Desorption efficiencies of Lead using 0.3 M HCl after adsorption of 200 ppm.

Adsorbent code	q_e adsorbed	q_e desorped	% desorption
MACS	155.0	126.27	81.46
MACL	134.0	117.40	87.62
ACS	33.9	30.54	90.08
ACL	30.9	28.64	92.68
DS	88.2	74.84	84.85
DL	64.7	56.17	86.82

Table 10: Desorption efficiencies of Lead using 0.6 M HCl after adsorption of 200 ppm.

Adsorbents	q_e (mg/g)	Ref.
DS	90.50	This work
DL	66.60	
ACS	36.00	
ACL	33.40	
MACS	175.63	
MACL	164.55	
Siderite Chitosan	8.58	[27]
Siderite	12.43	[26]
Rice husk ash	12.63	
Kaolinite clay	19.27	
Data pits carbon	30.66	

Table 11: Comparison of the adsorption capacities of Pb^{2+} onto various adsorbents.

Conclusion

Based on the results, it is clear that the Lead-removal values achieved with Nitric acid modified water hyacinth activated carbon were higher than those of dried water hyacinth and activated carbon due to the increase in the number of carboxylic groups on the surface of the modified activated carbon. The main advantages of this removal procedure include (i) simplicity, (ii) cost effectiveness, (iii) rapidity, and (iv) a higher removal efficiency of toxic mercury ions. Based upon the experimental results of this study, the following conclusions can be drawn: It was found that the sorption process is pH-dependent and the maximum adsorption capacity of Pb^{2+} is at pH 5. It was found that the extent of Pb^{2+} adsorption increases upon increasing initial concentration and contact time till reached to equilibrium. Pb^{2+} uptake almost remained constant after 60 min for MACS, MACL, ACS and ACL and after 90 min for DS and DL. The kinetic studies of lead adsorption onto DS, DL, ACS, ACL, MACS and MACL were performed based on pseudo first-order, pseudo second-order, and intra-particle diffusion. The data indicated that the adsorption kinetics of lead on all adsorbents followed the pseudo-second order model at different lead concentrations. The equilibrium data were analyzed using the Langmuir and Freundlich isotherms and the characteristic parameters for each isotherm were determined. The results showed that the experimental data were correlated reasonably well by the Langmuir isotherm model. Thermodynamic studies indicated that the adsorption process was an endothermic process. Desorption of Pb^{2+} using 0.6 M HCl as a desorping agent by disruption coordination of metal ions and subsequent release from the activated carbon surface into desorption medium was studied.

References

1. Momcilovic M, Purenović M, Bojić A, Zarubica A, Ranđelović M (2011) Removal of lead (II) ions from aqueous solutions by adsorption onto pine cone activated carbon. Desalination 276: 53-59.
2. Sreejalekshmi KG, Krishnan KA, Anirudhan TS (2009) Adsorption of Pb(II) and Pb(II)-citric acid on sawdust activated carbon: Kinetic and equilibrium isotherm studies. J Hazard Mater 161: 1506-1513.
3. Pollard SJT, Fowler GD, Sollars CJ, Perry R (1992) Low-cost adsorbents for waste and wastewater treatment: a review. Science of the total environment 116: 31-52.
4. Dagnall R, West T, Young P (1965) Determination of lead with 4-(2-pyridylazo)-resorcinol-I: Spectrophotometry and solvent extraction. Talanta 12: 583-588.
5. Ahmed MJ, Theydan SK (2012) Corrigendum to "Equilibrium isotherms and kinetics modeling of methylene blue adsorption on agricultural wastes-based activated carbons" [Fluid Phase Equilib 317 (2012) 9-14]. Fluid Phase Equilibria 318: 115.
6. Kennedy LJ, Vijaya JJ, Sekaran G (2005) Electrical conductivity study of porous carbon composite derived from rice husk. Materials chemistry and physics 91: 471-476.
7. Guo Y, Rockstraw DA (2006) Physical and chemical properties of carbons synthesized from xylan, cellulose, and Kraft lignin by H_3PO_4 activation. Carbon 44: 1464-1475.
8. Biniak S, Pakuła M, Szymański GS, Światkowski A (1999) Effect of activated carbon surface oxygen-and/or nitrogen-containing groups on adsorption of copper (II) ions from aqueous solution. Langmuir 15: 6117-6122.
9. Machida M, Kikuchi Y, Aikawa M, Tatsumoto H (2004) Kinetics of adsorption and desorption of Pb (II) in aqueous solution on activated carbon by two-site adsorption model. Colloids and Surfaces A: Physicochemical and Engineering Aspects 240: 179-186.
10. Aroua MK, Leong SP, Teo LY, Yin CY, Daud WM (2008) Real-time determination of kinetics of adsorption of lead(II) onto palm shell-based activated carbon using ion selective electrode. Bioresour Technol 99: 5786-5792.
11. Acharya J, Sahu JN, Mohanty CR, Meikap BC (2009) Removal of lead (II) from wastewater by activated carbon developed from *Tamarind wood* by zinc chloride activation. Chemical Engineering Journal 149: 249-262.
12. Boudrahem F, Aissani-Benissad F, Ait-Amar H (2009) Batch sorption dynamics and equilibrium for the removal of lead ions from aqueous phase using activated carbon developed from coffee residue activated with zinc chloride. Journal of environmental management 90: 3031-3039.
13. Dwivedi CP, Sahu JN, Mohanty CR, Mohan BR, Meikap BC (2008) Column performance of granular activated carbon packed bed for Pb(II) removal. J Hazard Mater 156: 596-603.
14. Ahmadpour A, Tahmasbi M, Bastami TR, Besharati JA (2009) Rapid removal of cobalt ion from aqueous solutions by almond green hull. J Hazard Mater 166: 925-930.
15. Demiral H, Demiral I, Tümsek F, Karabacakoğlu B (2008) Adsorption of chromium (VI) from aqueous solution by activated carbon derived from olive bagasse and applicability of different adsorption models. Chemical Engineering Journal 144: 188-196.
16. Pavan FA, Mazzocato AC, Gushikem Y (2008) Removal of methylene blue

dye from aqueous solutions by adsorption using yellow passion fruit peel as adsorbent. Bioresour Technol 99: 3162-3165.

17. Lagergren S (1898) Zur theorie der sogenannten adsorption gelöster stoffe.
18. Weber TW, Chakravorti RK (1974) Pore and solid diffusion models for fixed-bed adsorbers. AIChE Journal 20: 228-238.
19. Nuhoglu Y, Malkoc E (2009) Thermodynamic and kinetic studies for environmentaly friendly Ni(II) biosorption using waste pomace of olive oil factory. Bioresour Technol 100: 2375-2380.
20. Weber W, Morris J (1963) Kinetics of adsorption on carbon from solution. J Sanit Eng Div 89: 31-60.
21. Boyd GE, Adamson AW, Myers LS Jr (1947) The exchange adsorption of ions from aqueous solutions by organic zeolites; kinetics. J Am Chem Soc 69: 2836-2848.
22. Reichenberg D (1953) Properties of ion-exchange resins in relation to their structure. III. Kinetics of exchange. Journal of the American Chemical Society 75: 589-597.
23. Dural MU, Cavas L, Papageorgiouc SK, Katsaros FK (2011) Methylene blue adsorption on activated carbon prepared fromPosidonia oceanica (L.) dead leaves: Kinetics and equilibrium studies. Chemical Engineering Journal 168: 77-85.
24. Milonjic SK (2007) A consideration of the correct calculation of thermodynamic parameters of adsorption. J Serb Chem Soc 72: 1363-1367.
25. Rao MM, Rao GP, Seshaiah K, Choudary NV, Wang MC (2008) Activated carbon from Ceiba pentandra hulls, an agricultural waste, as an adsorbent in the removal of lead and zinc from aqueous solutions. Waste Manag 28: 849-858.
26. Mohammadi SZ, Karimi MA, Afzali D, Mansouri F (2010) Removal of Pb (II) from aqueous solutions using activated carbon from Sea-buckthorn stones by chemical activation. Desalination 262: 86-93.
27. Giraldo-Gutiérrez L, Moreno-Piraján JC (2008) Pb (II) and Cr (VI) adsorption from aqueous solution on activated carbons obtained from sugar cane husk and sawdust. Journal of Analytical and Applied Pyrolysis 81: 278-284.